Planet. Space Sci. 1970, Vol. 18, pp. 953 to 964. Pergamon Press. Printed in Northern Ireland

METEOROID IMPACTS ON THE GEMINI WINDOWS

HERBERT A. ZOOK, ROBERT E. FLAHERTY and DONALD J. KESSLER
Space Physics Division, NASA Manned Spacecraft Center, Houston, Texas 77058, U.S.A.

(*Received* 10 *November* 1969)

Abstract—Fourteen windows of the Gemini spacecraft were closely examined after return from space flight for evidence of meteoroid impact. Although a number of microscopic pits were found on each window, only one of these pits appears to have been caused by a meteoroid impact. A meteoroid flux-mass relation calculated from this single hit is found to be in close agreement with Naumann's (1966) analysis of the Explorer and Pegasus meteoroid penetration experiments. Particle, mass, and area distribution curves are derived from the flux-mass relation and are presented in graphical form. Problems in interpreting the data because of contaminants on the windows are also discussed.

1. INTRODUCTION

The windows of the 10 manned Gemini spacecraft that were orbited during 1965 and 1966 presented an excellent opportunity to search for meteoroid impact evidence and thereby to determine the associated meteoroid impact rate. The opportunity was good because the windows* presented a smooth exterior surface that facilitated detection of very small impact craters and because the area-time product of 42·8 ft²-days in space for the 14 windows examined was quite adequate to determine answers to certain questions raised by previous experimental results about the influx rate of micrometeoroids.

Two problems did arise, however, in interpreting the results from this experiment. First, postflight examination of the windows revealed a number of microscopic pits on both the interior and exterior surfaces of the windows. Therefore, it was necessary to distinguish between craters that were caused by impacting meteoroids and pits that were caused by other sources. Second, after the spacecraft had returned from space, a somewhat scaly substance was found adhering to portions of the windows and occasionally covering as much as 80 per cent of the window surface. The thickness of the scale varied from a fraction of a micron to as much as 50 μ. Obviously, if this material was on the windows while in orbit, it would significantly modify the resulting analysis of the meteoroid influx rate; for example, micron-sized meteoroids would not penetrate the thicker scale and hence would not be detected on portions of the windows.

The following sections contain: (2) A discussion of the window contamination problem; (3) A description of the experimental procedure used to examine the windows; (4) An analysis of how the window data are related to laboratory tests; (5) A discussion of the probable validity of the Gemini window data; (6) A presentation of the cumulative flux vs. mass; (7) Additional results of interest derived from the meteoroid impact experiments; (8) Conclusions.

2. WINDOW CONTAMINATION

All of the Gemini windows were found to have been contaminated to varying degrees with foreign material during space flight. The source of this contamination is still a matter of some conjecture. However, a credible reconstruction of the events that caused the scale on the windows has been derived and, because of its pertinence to the subject of this paper, is presented briefly in the following paragraphs.†

* Only the outer pane of the three-pane Gemini window was considered in this examination.

† This reconstruction was transmitted to us by G. P. Bonner of the Astronomy Branch and others at the NASA Manned Spacecraft Center.

After the spacecraft returned from space, samples of the scale from several windows were chemically analyzed (Bonner *et al.*, 1968). The major constituent of the scale was found to be a silicon oil. The presence of a transparent, oily material on some spacecraft windows during the orbital period became apparent during the GT-IV flight. During extra-vehicular activity in this flight, the pilot inadvertently brushed against and smeared the window. The smearing was observed and reported by the command pilot and is also apparent in a photograph taken of the GT-IV window while in orbit. These observations led to the speculation that the oil was released from the ablative nose-cone fairing which protected the nose of the Gemini spacecraft from aerodynamic heating during launch. It seemed quite possible that the DC-325 ablation material would heat enough during launch to release silicon oil in a liquid form that could then wash back onto the windows.

For this reason, the outer windows of Gemini spacecraft VIII through XII were protected during launch with an additional covering window which was discarded, as was the nose-cone fairing, after orbit insertion. This precaution, however, only partially reduced the window contamination (large variations in contamination from window to window made it somewhat difficult to correlate changes in contamination with actions taken to reduce contamination). Other speculations concerning additional sources of contamination were offered and found lacking in one respect or another.

It was later noted that oil occasionally appeared on the inside as well as the outside of the outer Gemini windowpanes. This observation led to the proposition that silicon oil had escaped from the potting material (RTV-90) which was used as a seal for the window frames and had spread onto the surface of the glass. To verify this proposition, the GT-XII windows were baked in an oven under vacuum conditions before flight and were cleaned before launch. These windows did exhibit significantly less contamination after recovery than did the windows of the previous Gemini spacecraft.

Hence, the following Gemini window contamination history is widely accepted. Silicon oil from the RTV-90 potting compound creeps out onto the surface of the window under the vacuum conditions of space. Vacuum grease from the window gasket (a paper material saturated with vacuum grease) may also do the same. Silicon oil from the ablative nose-cone fairing quite probably also gets on the windows during launch unless the windows have protective covers. During reentry, material from the rear ablative heat shield (also DC-325) as well as material from some of the guillotined electrical connections (the unique compositional elements of which were detected in the chemical analysis of the window scale) swirls back upon the window and adheres to the silicon oil already on the window. The heat of reentry then bakes this material firmly on the window, producing the scale observed upon recovery. A closer look at how this contamination affects the meteoroid impact analysis is deferred to Section 5.

3. EXPERIMENTAL PROCEDURE

After a small sample of the window scale was removed for chemical analysis, the windows were subjected to an optical analysis to determine the change in optical properties caused by the contamination. The scale was then scraped off with a razor blade, and the window surfaces were cleaned and subjected to a second optical analysis. The windows were then examined in detail for evidence of meteoroid impact cratering. It should be noted at this time that, although great care was exercised, it is difficult to be certain whether or not the razor-blade cleaning was responsible for any of the pits later observed on the windows. It is believed, however, that no particular problem is presented with respect to confusing this type pit with impact craters, as will be explained in Section 4.

Selected regions of several windows (both the exterior and interior surfaces) were scanned

at a magnification of 100× and all pits were recorded that had diameters larger than 20 μ. Between four and ten 20-μ or larger craters per in^2 were found on the outside of the windows, and between one and six of these craters were found on the inside of the windows. Roughly, there were twice as many pits of this size on the outside surfaces as on the inside surfaces.

The entire surface (85 in^2) of each window was then scanned at a magnification of 20×, and all craters were recorded that had diameters larger than 100 μ. All of these craters and some of the smaller ones were then examined in detail at magnifications up to 750×. Although there is considerable variation among individual pits, the ratio of pit diameter to pit depth was typically about 10, regardless of crater size. Similar results for Vycor glass were found for craters produced in the laboratory at both high and low impact velocities.

4. ANALYSIS OF DATA

The flight time in days and the number of pits 100 μ or larger in dia. that were found on each window examined are shown in Table 1. It is seen that the correlation between length of space flight and number of pits on the windows is not close. For example, GT-VII was in orbit for 13·8 days and had 16 and 15 pits on the outside surfaces of the left and right windows, respectively, while GT-VIA had corresponding numbers of 21 and 9 pits but was only in orbit for 1·1 days of flight. Curiously, there were few 100-μ and larger craters on the interior surfaces of the windows; two or three per window was typical.

TABLE 1. NUMBER OF PITS WITH DIAMETERS LARGER THAN 100 μ ON THE GEMINI WINDOWS

Spacecraft	Exposure (days)	Number of pits	
		Left window	Right window
GT-IV	4·1	2	6
GT-V	7·9	4	14
GT-VIA	1·1	21	9
GT-VII	13·8	16	15
GT-IX	3·0	7	3
GT-X	2·9	9	9
GT-XI	3·0	NA	10
GT-XII	3·9	NA	3

The pit data could be analyzed by subtracting the number of pits observed on the inside of the windows from those observed on the outside and ascribing the difference to meteoroid impact cratering. This method is not satisfactory for at least four reasons:

(1) The GT-VIA mission, for example, would give an average formation rate for the 100-μ and larger craters about 10 times greater than would be obtained from the GT-VII mission. This would indicate considerable shower activity for the very small meteoroids ($\sim 10^{-10}$ g). Radio meteor data indicate that major shower activity decreases significantly relative to sporadic activity as the meteoroid mass decreases. The trend indicated by the radio meteor data would predict little detectable shower activity at 10^{-10} g. This trend is confirmed by the penetration histories of the Explorer and Pegasus penetration satellites. Also, the GT-VII and GT-VIA spacecraft were in orbit at the same time.

(2) The left and right windows of several of the spacecraft do not have similar numbers of 100-μ and larger craters. The chance occurrence of such large discrepancies is very small.

(3) For the 20-μ-dia. and larger craters, one window was examined which had about the same density of pits (approximately 6 per in^2) on the inside of the window as on the outside.

And, in general, for the 20-μ craters, the difference between the outside and inside crater densities varied greatly from 0 per in^2 to about 5 per in^2. This difference also had no particular correlation with the length of space flight.

(4) With one exception, the pits observed on the windows do not have the characteristics of laboratory-produced hypervelocity impacts by small projectiles. The overwhelming majority of the pits closely resembles the type of pit that is commonly left after a glass-polishing operation.

The last reason cited above provides the only reasonable criterion found for determining whether or not a Gemini window pit is, in fact, a meteoroid impact crater. That is, the overwhelming proportion of meteoroids striking the spacecraft should have velocities in excess of 7 km/sec (the minimum possible velocity of impact equals the escape velocity minus the orbital velocity $\approx$4 km/sec). Craters produced in Vycor glass in the laboratory by projectiles traveling 7 km/sec or faster have a characteristic molten-appearing or partly fused region in the central part of the crater. This fused appearance in the central portion of the crater or pit has never been observed for low-velocity impact craters and for chip-outs or pits left from a glass-polishing process. The kinds of pits found on the windows and the impact craters produced in the laboratory will be examined and compared in the following paragraphs.

The single crater found on the Gemini windows that is believed to be caused by meteoroid impact was found on the left-hand window of the GT-V spacecraft and is shown in Fig. 1. The crater is $\sim$110 μ in dia. and 12 μ deep and has many of the characteristics of a hypervelocity impact in this size range. That is, there is a molten-appearing raised lip surrounding the indented central region of the crater. Exterior to this region and roughly concentric to it is a conchoidal fracture region. (The crater diameter referred to henceforth will be the diameter of the conchoidal fracture region unless otherwise specified.) The glass in the conchoidal fracture region has chipped away to a depth of $\sim$5 μ. Figure 2 illustrates a cross-sectional view of this crater (not to scale).

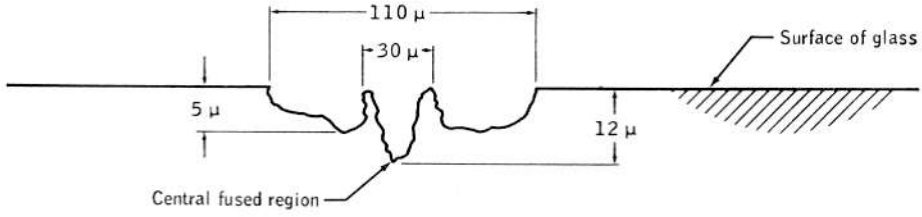

FIG. 2. APPROXIMATE CROSS-SECTIONAL PROFILE OF THE GT-V METEOROID IMPACT CRATER.

Because GT-VII spent the longest time in space, the pits or craters on its windows are of unusual interest. Each of the 31 100-μ and larger pits was examined in great detail at magnifications up to 750$\times$ to search for evidence of hypervelocity impact. Typical examples of pits on the GT-VII windows are shown in Figs. 3–6. Figure 3 shows a chip-out or pit $\sim$90 μ in dia. and $\sim$10 μ deep. A small satellite crater is located nearby and just out of the field of view in the photograph. One or more small satellite craters were associated with a large fraction of the Gemini window craters. Crater grouping is a common occurrence for pits made during polishing.

Figure 4 shows an elongated crater of lateral dimensions 100 μ by 130 μ and $\sim$10 μ deep. A small satellite crater is located nearby. Figure 5 shows a third chip-out $\sim$120 in dia. and again $\sim$10 μ deep.

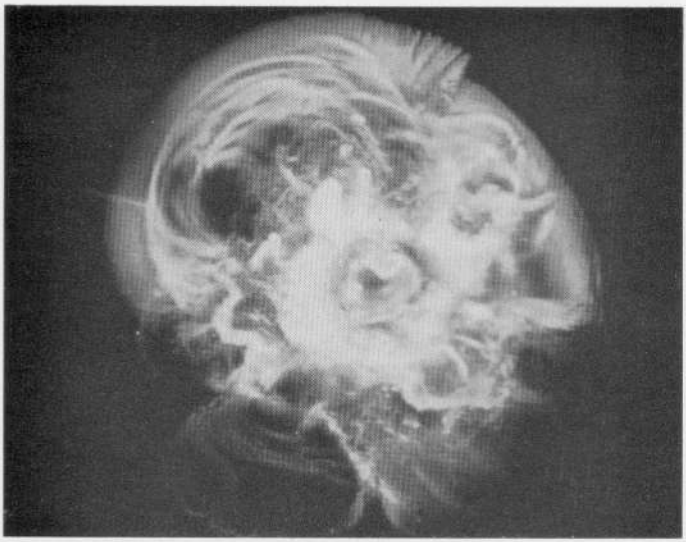

FIG. 1. POSTULATED METEOROID IMPACT CRATER ON THE LEFT-HAND GT-V WINDOW.
Crater diameter is $\sim 110\ \mu$ and crater depth is $12\ \mu$.

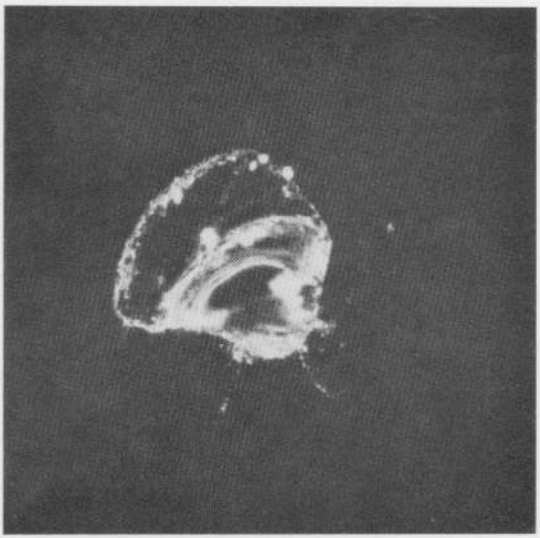

FIG. 3. CHIP-OUT ON A GT-VII WINDOW.
The diameter is $\sim 90\ \mu$ and the depth is $\sim 10\ \mu$.

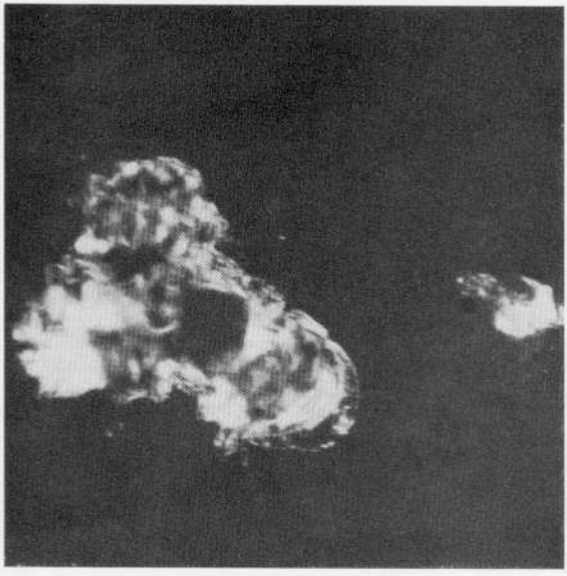

FIG. 4. CHIP-OUT ON A GT-VII WINDOW.
The diameter is $\sim 110\ \mu$ and the depth is $\sim 10\ \mu$.

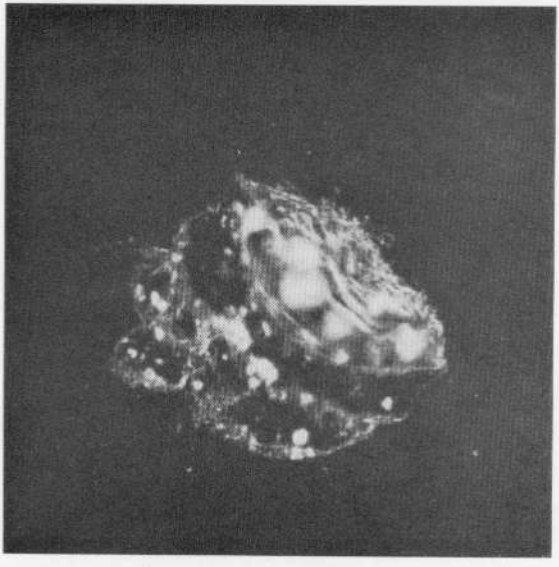

FIG. 5. CHIP-OUT ON A GT-VII WINDOW.
The diameter is $\sim 120\ \mu$ and the depth is $\sim 10\ \mu$.

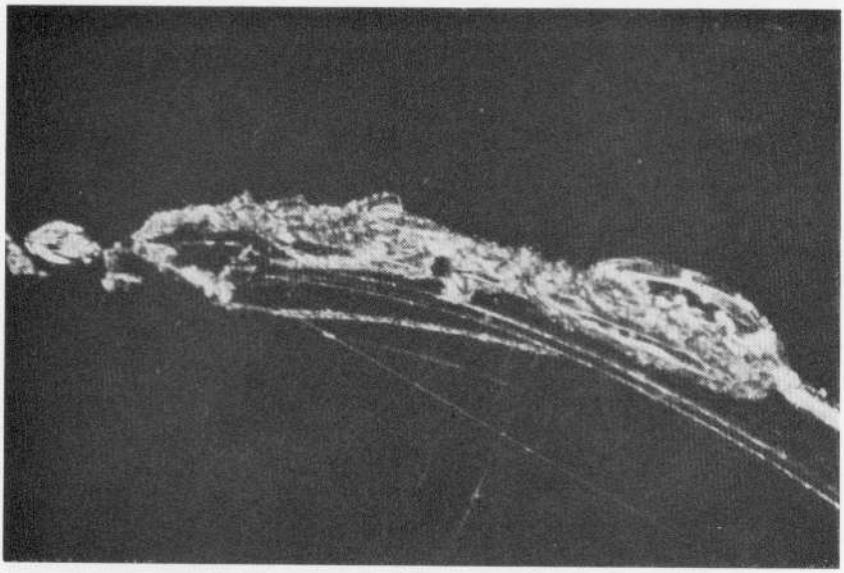

FIG. 6. SCRATCH ON A GT-VII WINDOW.

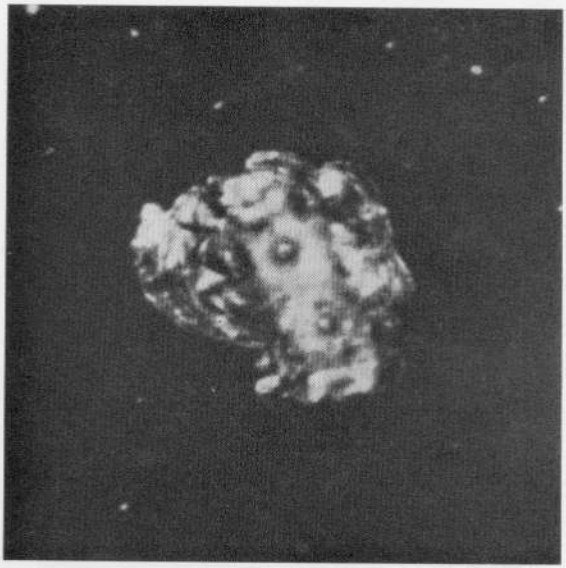

FIG 7. TWO IMPACT CRATERS PRODUCED AT THE DRAG-ACCELERATING FACILITY OF THE MARTIN COMPANY.
The diameter of the smaller crater is ~100 μ and the depth is ~13 μ. The diameter of the larger crater is ~200 μ and the depth is ~14 μ.

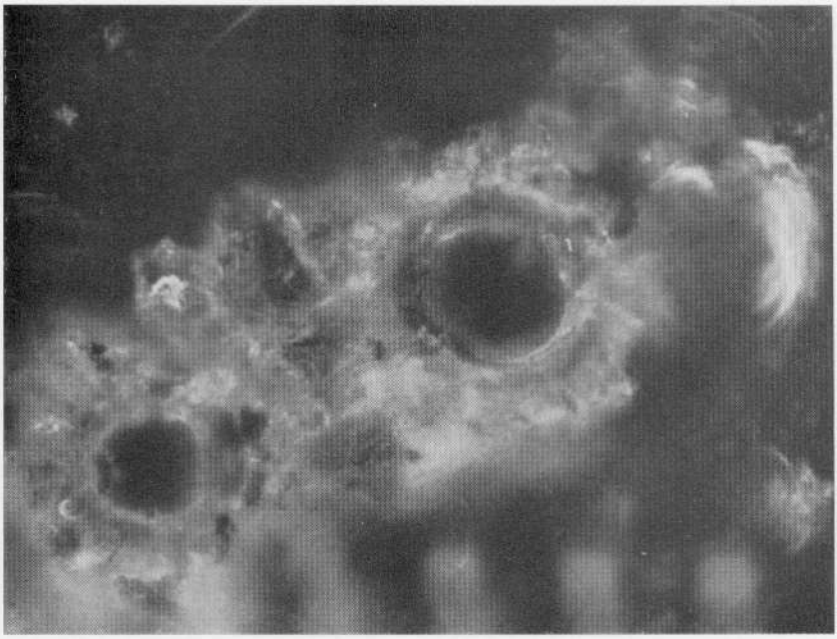

FIG. 8. THE TWO CRATERS OF FIG. 7 SHOWN AT A HIGHER MAGNIFICATION TO ILLUSTRATE THE MOLTEN-APPEARING CENTRAL REGIONS.
The lip diameters of the craters are ~20 μ (smaller) and ~30 μ (larger).

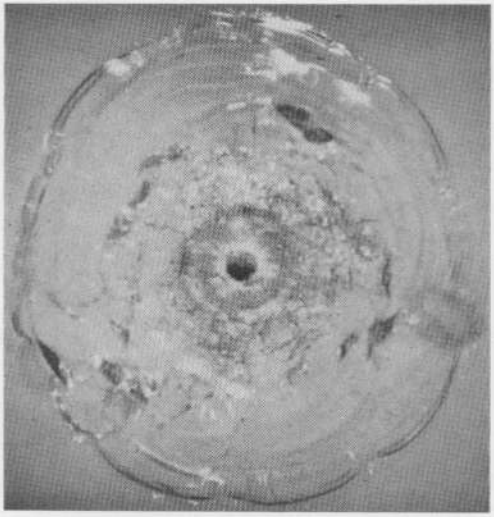

FIG. 9. IMPACT CRATER CAUSED BY A 384-μ-DIA. PYREX SPHERE IMPACTING INTO VYCOR AT A VELOCITY OF 7·37 km/sec.
The diameter of the crater (including the spalled-out region) is ~8600 μ.

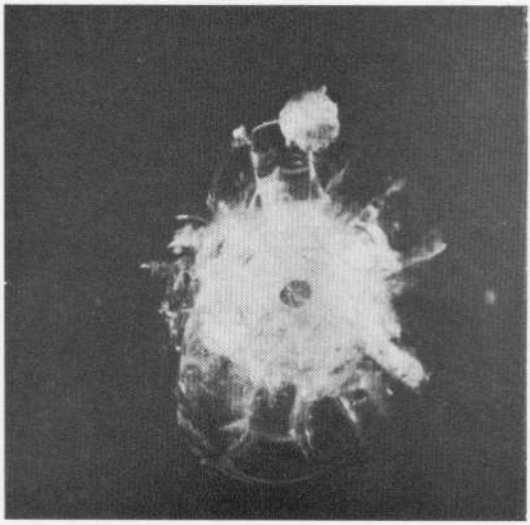

FIG. 10. IMPACT CRATER CAUSED BY A $\frac{1}{16}$-in.-DIA. ($\approx 1600\,\mu$) GLASS SPHERE IMPACTED INTO VYCOR AT A VELOCITY OF 0·37 km/sec.
The crater diameter is $\sim 1400\,\mu$.

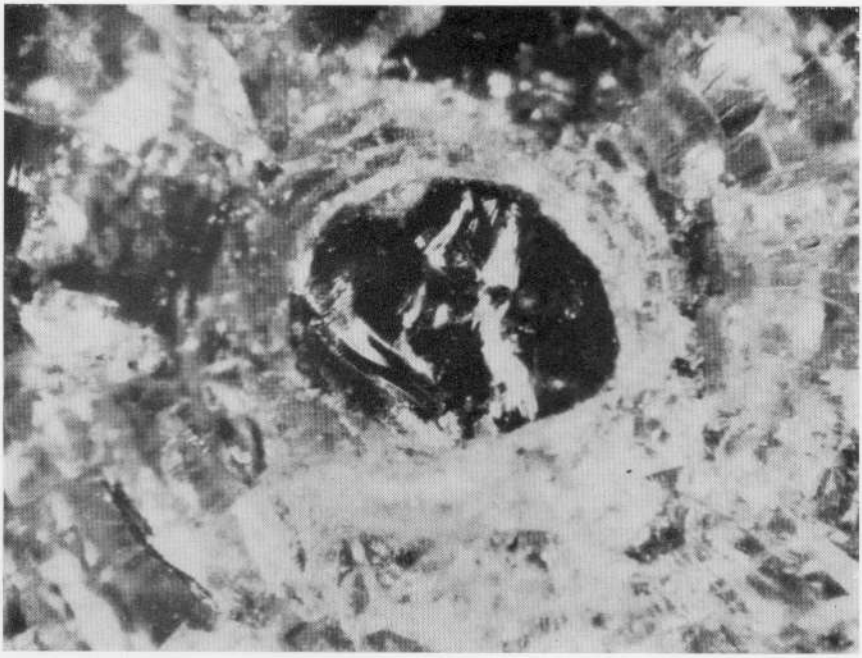

FIG. 11. CENTRAL PORTION OF CRATER IN FIG. 10 SHOWN AT HIGHER MAGNIFICATION.
The diameter of the relatively unbroken central region is $\sim 120\,\mu$.

Scratches are another type of imperfection, of which several are included among the 100-μ and larger pits listed in Table 1. A very large scratch that is several hundred microns long but only a few microns deep and 70 or 80 μ wide is shown in Fig. 6. This scratch was one of the two imperfections in the GT-VII windows that had a linear dimension over 200 μ. Occasionally, a chip-out was seen that was not immediately identifiable as being of non-hypervelocity impact origin. However, detailed studies of these craters revealed no molten-appearing central region where the glass appeared to have flowed under impact heating. The GT-V crater previously mentioned was, of course, the single exception.

Figure 7 shows two hypervelocity impacts into Vycor glass (Corning 7913) that were produced with the exploding lithium-wire drag-accelerating gun of the Martin Company. Glass spheres $\sim$60 μ in dia. were used as projectiles but these generally broke into smaller pieces upon launch. The two craters were made by fragments that were, perhaps, between 4 and 5 μ in dia. Some of the craters obtained at the Martin facility did not show the striking molten-appearing central region and were assumed to be caused by trash that came down later at a slower velocity. Indicated velocities on some of the faster projectiles ranged up to 20 km/sec. Craters that have the molten-appearing central regions were assumed to be caused by the very fast projectiles because it has not been possible to produce this type of crater by any other means.

Figure 8 shows the central regions of the same two craters at a higher magnification and illustrates how strikingly evident it is that the central region once consisted of glass flowing in the molten state. (Note: The two craters shown are typical of dozens of the Martin craters. These were fortunately close enough together to exhibit both in a single photograph. These two craters are also interesting because they are in the same size range and are similar in appearance to the GT-V crater.)

Figure 9 shows the results of a 384-μ-dia. Pyrex projectile impacted into Vycor at 7·37 km/sec. The crater is $\sim$8600 μ (0·86 cm) in dia. and 800 μ deep. The glass around and close to the impact point appears to have been shattered and partly fused, indicating considerable heat production during the impact. In general, evidence of melting is conspicuously present at impact velocities above 7 km/sec for glass projectiles. Below this velocity, although the glass appears highly crushed at the impact point, melting is not so evident. At much lower impact velocities, there is no evidence of melting at the impact point.

Figure 10 shows the results of a $\frac{1}{16}$-in.-dia. glass projectile impacted into Vycor at $\sim$370 m/sec—a low-velocity impact. The central region of this crater is shown at higher magnification in Fig. 11. The shattered glass is blocky and angular and shows none of the evidence of fusion that is apparent in Figs. 7–9.

5. DISCUSSION OF EXPERIMENTAL RESULTS

When the pits on the Gemini windows are compared with craters produced under experimental conditions in Vycor glass at both high and low velocities, it is seen that the Gemini window pits do not even faintly resemble craters made by hypervelocity impacts (with the one exception noted on the GT-V window). The Gemini window pits do not even resemble craters made by impacting projectiles at intermediate and low velocities, although the resemblance would improve if all of the incipient spall and crushed glass were removed from the low-velocity impact craters. The pits on the Gemini windows do resemble one class of pits very closely; namely those left by the glass-polishing process. One may then ask why there are significantly more pits on the outside of the windows than on the inside. There is no certain answer to this question. It has been found, however, that by gouging at very

minute postpolish pits with a pin, one can often substantially enlarge them to the point that they would appear very similar to the 100-μ and larger pits on the windows. The reentry heating and later scraping with a razor blade could have produced some of the pits observed on the exterior surfaces. Although not all of the 20-μ and larger diameter craters were exhaustively examined because of the prohibitively large number of them, the observations previously mentioned also apply to the smaller craters that were so examined.

The question now arises whether or not the contamination on the windows has hidden or disguised impacts of very small meteoroids. It is not possible to be certain but an educated guess can be made based on the window contamination history previously postulated. Because a film of silicon oil from the window seals appears to be the major (and on GT-8 through GT-12 perhaps the only) source of window contamination while in orbit, the thickness of the oil contamination should be greater near the edge of the windows than the center. After reentry, the baked-on scale was observed to be thicker near the edge of some of the windows. In fact, central regions of many of the returned windows were entirely free of scale, and impact characteristics of micron-sized meteoroids would not be modified if these window areas were similarly clean in space. Impacts created by larger meteoroids would, of course, be less affected by a thin film. Hence, it seems reasonable to assume that a significant fraction (perhaps one-half) of the windows was not contaminated severely enough to disguise impacts made by meteoroids with diameters as small as 4 μ. A 4-μ meteoroid, traveling at 20 km/sec, should produce a crater in Vycor $\sim$100 μ in dia. The detection threshold set on the Gemini windows was 100 μ. It will therefore be assumed in the following analysis that exactly one-half of the window surface was available for undistorted meteoroid impacts producing craters 100 μ and larger in dia.

6. FLUX OBTAINED FROM METEOROID IMPACT DATA

To obtain the flux of particles down to the threshold size, the single impact is divided by the exposed area-time of 3·98 m^2-days (or 42·8 ft^2-days), divided by 0·63 to allow for Earth shielding appropriate to the Gemini flights, and multiplied by 2 to account for the assumed effect of contamination. The result is approximately 0·8 meteoroid impacts per m^2-day of sufficient size to produce a crater in Vycor at least 100 μ in dia.

The mass of a meteoroid causing a crater in Vycor 100 μ in dia. must be estimated by extrapolating lower-velocity larger-mass laboratory data. The results of impacting Pyrex spheres 384 μ in dia. into sections of the GT-V window (made of Vycor) are given in Table 2. The projectiles were quite uniform, varying from the mean by less than 5 μ in dia. and 1 μg in mass. The average projectile mass was 63·1 μg and the corresponding average density was 2·13 g/cm^3.

TABLE 2. IMPACT DATA OBTAINED WITH A LIGHT-GAS GUN*

P (μ)	V (km/sec)	P/d	D (μ)	D/P
807	7·41	2·10	6747	8·36
786	7·37	2·05	7248	9·22
790	7·38	2·06	7960	10·08
800	7·37	2·08	8582	10·73
788	7·4 (est.)	2·05	7265	9·22
798	7·34	2·08	7176	8·99
799	7·34	2·08	8913	11·16

* Penetration depth, P, impact velocity, V, ratio of penetration depth to projectile diameter, P/d, crater diameter, D, and ratio of crater diameter to penetration depth, D/P, respectively, for 384-μ-dia. Pyrex projectiles impacting Vycor glass.

The Manned Spacecraft Center empirical penetration formula is used to extrapolate from laboratory velocities and densities to an average meteoroid impact velocity and an average meteoroid mass. The equation is

$$P/d = \text{const}\, d^{1/18}\rho_p^{1/2}(V\cos\theta)^{2/3}$$

where P is the depth of penetration in cm, d is the equivalent projectile diameter in cm, ρ_p is the projectile density in g/cm^3, V is the projectile velocity in km/sec, and θ is the angle of incidence. The constant is evaluated from the data in Table 2 for Vycor and is 0·45.

Dohnanyi (1966) derived the distribution in velocity of meteoroids at the top of the Earth's atmosphere from an analysis of photographic meteor observations. This distribution is given by

$$n(V) = \begin{cases} cV^{1.6} & 11{\cdot}2 \leq V \leq 16{\cdot}6 \text{ km/sec} \\ 1{\cdot}61 \,.\, 10^7 cV^{-4.3} & 16{\cdot}6 < V < 72{\cdot}2 \text{ km/sec} \end{cases}$$

where c is the normalization constant. The corresponding average velocity is 19·17 km/sec. Naumann (1966) has adopted the velocity distribution of Dohnanyi as appropriate for small meteoroids detected by the Pegasus and Explorer penetration satellites. He also used the meteoroid mass density distribution (somewhat modified) of Verniani and Hawkins (1965) which they obtained from radar meteor observations. The modified distribution used was as follows: 51 per cent of the meteoroids have a density of 0·37 g/cm^3, 45 per cent have a density of 2·8 g/cm^3, and 4 per cent have a density of 8 g/cm^3. These distributions and averages are assumed appropriate for the Gemini window penetration data. Normal impact will be assumed so that $\cos\theta = 1$.

The average value of D/P from the data in Table 2 is 9·7, hence a 100-μ-dia. crater corresponds to a 10·3-μ-deep crater. Using the average values above for meteoroids, this crater would be produced by a meteoroid with a diameter of 3·72 μ and a mass of 4·77 . 10^{-11} g. The D/P values do not depend very much on crater size, as shown by the data in Table 3.

TABLE 3. IMPACT DATA OBTAINED AT THE MARTIN COMPANY*

P (μ)	D (μ)	D/P
28	400	14·38
20	170	8·50
15	150	10·0
25	220	8·80
18	170	9·44
8	55	6·87
10	130	13·0
150	1050	7·00
65	700	10·77
62	350	5·76
66	550	8·33
42	400	9·52
31	200	6·45

* Penetration depth, crater diameter, and the ratio of these two, respectively, for impacts of high-velocity glass fragments into Vycor.

These data were taken from all of the hypervelocity-appearing craters on four separate targets impacted at the Martin Company hypervelocity facility. There is a fair amount of

scatter in the D/P data which is probably caused by the irregular-shaped projectiles. The average of the D/P data in Table 3 is 9·1, which does not differ greatly from the 9·7 value in Table 2. The latter value is assumed to apply to the Gemini windows.

The point defined by the flux* and meteoroid mass derived in the previous paragraph is shown with 95 per cent statistical confidence bars in Fig. 12 where the logarithm of the cumulative flux of particles having mass m or larger is plotted vs. the logarithm of the mass. Since no meteoroids impacted on the uncontaminated window surface that caused craters deeper than the single 12-μ-deep crater on the GT-V window (corresponding to a meteoroid diameter of 4·3 μ and a mass of $7{\cdot}4 \cdot 10^{-11}$ g), a 95 per cent statistical confidence level is used to establish a reasonable upper limit to the flux of meteoroids larger than this mass. The other points shown on the smooth curve are the Explorer and Pegasus penetration data as reduced by Naumann (1966) at the Marshall Space Flight Center and labeled 'fit II' in his report.

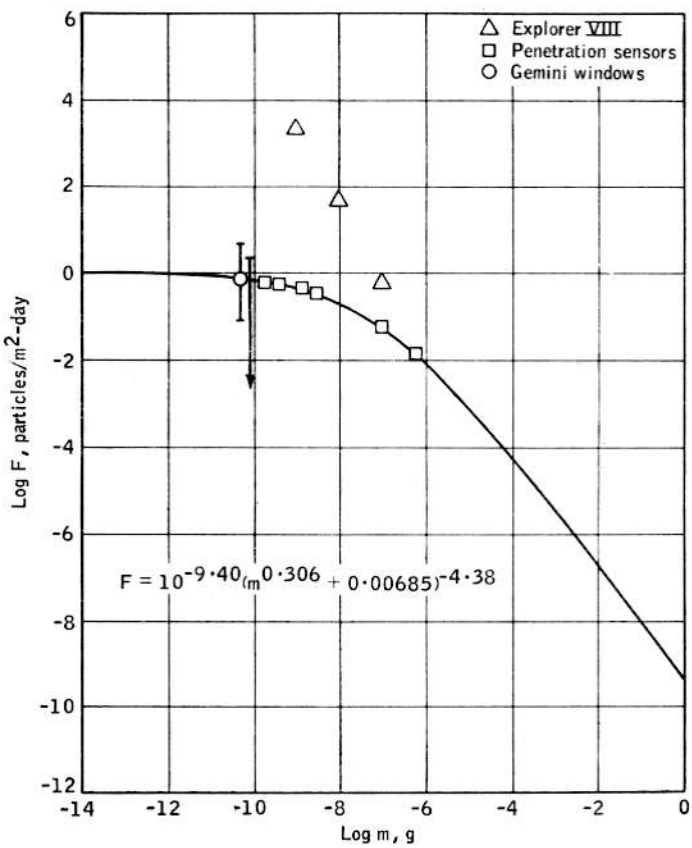

FIG. 12. LOG F (CUMULATIVE FLUX) VS. LOG m (METEOROID MASS).
The arrow indicates no impacts larger than the indicated mass (see text).

The smooth curve is defined by the analytical expression shown in Fig. 12. The parameters in this expression have been adjusted to fit the Pegasus and Explorer flux-mass points as reduced by Naumann and to extrapolate smoothly, at larger meteoroid masses, into the

* The flux correction factor given by Naumann (1966), which allows for meteoroids impacting at oblique angles and with velocities and densities different from average values, is ~10 per cent and is neglected.

meteoroid flux-mass curve adopted by Whipple (1963). The average mass density of the larger photographic meteoroids was arbitrarily chosen to be 0·4 g/cm³ so that Whipple's Equation (5) becomes

$$\log F = -1{\cdot}34 \log m - 9{\cdot}4$$

where F is the flux of particles incident from 2π sterad. of meteoroids of mass m gm and larger. It is seen that the flux-mass point determined from the Gemini windows is in excellent agreement with the Pegasus and Explorer penetration data.

The Explorer VIII acoustic data (McCracken, Alexander and Dubin, 1961) is in serious disagreement with the penetration and window data. Although not shown in Fig. 12, the Ariel II data (Jennison, McDonnell and Rodgers, 1967) support the penetration data. We believe the penetration data to be much more reliable than the acoustic data and, therefore, do not use the acoustic data to influence the shape of the cumulative flux-mass curve.

7. ADDITIONAL RESULTS OF INTEREST

Once a cumulative flux-mass curve is obtained, various distribution curves of interest may be derived. The derivative of F with respect to log m is plotted vs. log m in Fig. 13.

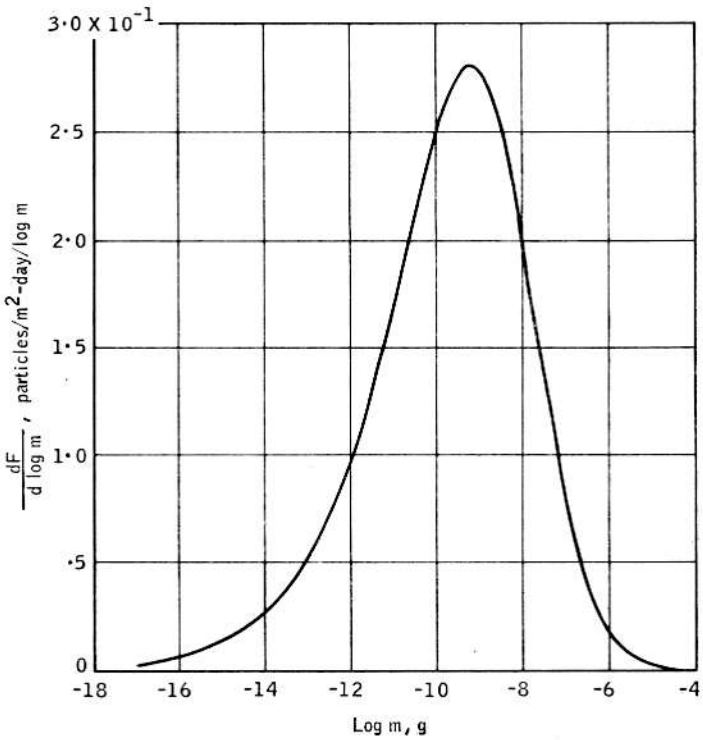

FIG. 13. THE DISTRIBUTION OF PARTICLES AS A FUNCTION OF LOG m.

The logarithmic derivative gives the distribution of particles as a function of log m and is convenient for graphical representation. The area under this curve is equal to the total number of meteoroids arriving at the surface of the Earth per m²-day. This curve peaks, on

a logarithmic mass interval, at about $10^{-9.2}$ g. The Pegasus and Explorer data have determined only the right side of the curve up to about 10^{-9} g. The left side of the curve is obtained by extrapolating the analytical function introduced in Fig. 12.

The distribution in mass of the incoming meteoroids as a function of log m is shown in Fig. 14. The area under the curve is equal to the total mass impacting the surface of the

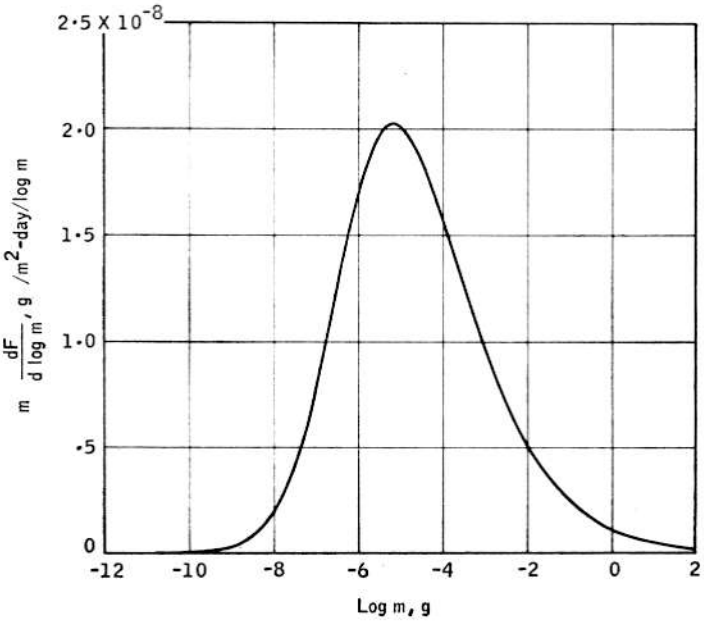

FIG. 14. THE DISTRIBUTION OF MASS AS A FUNCTION OF LOG m.

Earth per m²-day. The value is $8{\cdot}3 \times 10^{-8}$ g/m²-days which is almost identical to Whipple's 1967 estimate. This corresponds to about 48 tons of meteoritic material being collected by the Earth each day. The curve peaks at about $10^{-5.2}$ g with significant contributions from meteoroids with masses between 10^{-9} and 10 g. The photographic data (not including the Prairie Network data) have determined the right side of this curve, and the Pegasus and Explorer points have determined the left side. The region under this curve represents the mass region that is primarily responsible for mass transport in the lunar-erosion process. This observation follows from the work of Gault, Shoemaker and Moore (1963), in which they established that the mass of secondary ejecta produced by a hypervelocity impact is very nearly proportional to the mass of the incoming primary meteoroid. It is clear that, because of the generally small impacting masses involved, most of the impacts responsible for lunar erosion do not produce craters visible in the Lunar Orbiter photographs.

The distribution in cross-sectional area of incoming meteoroids as a function of log m is given in Fig. 15. Because the linear dimension of an impact crater in Vycor is related to the impacting meteoroid by the ratio $100/3{\cdot}7 = 27$, the area of a Vycor crater is related to the cross-sectional area of the impacting meteoroid by the ratio 730. Hence, by summing under the curve in Fig. 15, the cross-sectional area of meteoroids arriving per m²-day is obtained and is $9{\cdot}07 \times 10^{-6}$ cm²/m²-days. By multiplying by 730, the total area of chipped region being produced on unprotected Vycor glass per m²-day is derived. This area is $6{\cdot}62 \times$

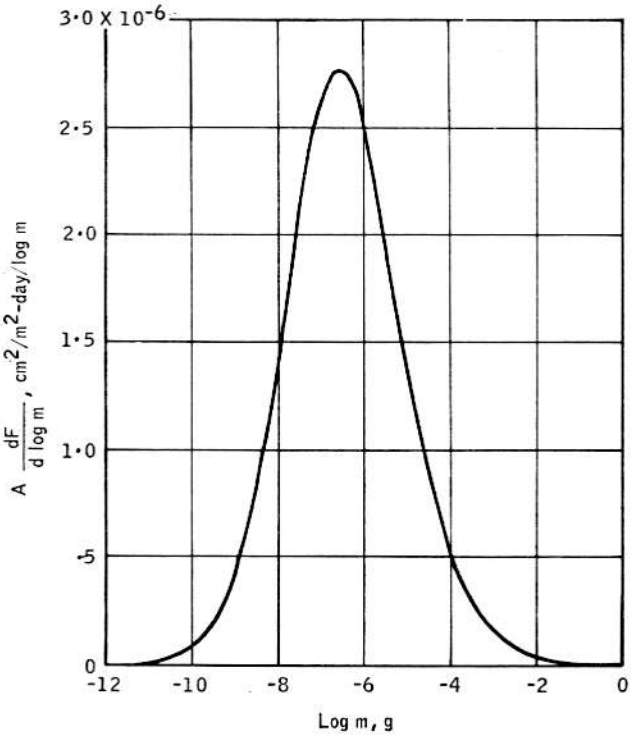

FIG. 15. THE DISTRIBUTION OF AREA AS A FUNCTION OF LOG m.

10^{-3} cm²/m²-days, which corresponds to an erosion rate of 2·4 per cent per hundred years on Vycor. Fused silica chips out to a somewhat larger diameter than does Vycor; nevertheless, meteoritic erosion in space on an unprotected glass surface, such as a telescope mirror, does not appear to be a serious problem. A catastrophic impact, causing the mirror to break, may be more likely to limit the lifetime of a space telescope.

The flux of meteoroids impacting the surface of the Earth (at the top of the atmosphere) at velocity V_∞ is decreased at 1 a.u., away from the Earth, by the factor $1 - V_e^2/V_\infty^2$ where V_e is the escape velocity from the surface of the Earth and V_∞ is the velocity of the meteoroid as measured at the top of the atmosphere. To arrive at the distribution of particles, area, or mass per unit volume at 1 a.u., it is necessary to multiply the gravitational decrease factor above by $4/(V_\infty^2 - V_e^2)^{1/2}$, integrate over the velocity distribution given by Dohnanyi (1966), and multiply by the ordinate of the appropriate distribution function in Figs. 13–15. The factor of 4 results from averaging the flux over 4π steradians to arrive at the above spatial densities. The number of particles per cm³, the cross-sectional area per cm³, and the mass per cm³ provided by meteoroids at 1 a.u. and in the ecliptic plane are obtained by summing over the distribution functions and are shown in Table 4.

TABLE 4. METEOROID PROPERTIES PER UNIT VOLUME AT 1 a.u. FROM THE SUN

Particles/cm³	Area (cm²/cm³)	Mass (g/cm³)
$2{\cdot}2 \times 10^{-15}$	$1{\cdot}6 \times 10^{-20}$	$1{\cdot}5 \times 10^{-22}$

Integration over the area distribution curve can be combined with an albedo to compare it with experimental observations of the zodiacal light. In particular, if it is assumed that the spatial density of meteoroids decreases as $r^{-1.5}$ where r is the distance from the Sun, a geometric albedo of 0·057 must be assumed to make the zodiacal light and penetration measurements agree. This is not an unreasonable value of geometric albedo for certain types of dust grains. The geometric albedo for asteroids ranges from 0·1 to 0·4.

8. CONCLUSIONS

The Gemini spacecraft windows have furnished an independent measurement of the near-Earth penetration flux for very small meteoroid masses. The contamination on the windows has made them less than ideal meteoroid detectors, but the contamination evidence does suggest that a reasonable fraction of the total window area was not coated while in orbit. This gives some, though not complete, confidence that the true Gemini flux lies within the 95 per cent statistical confidence bars shown in Fig. 12. The meteoroid flux obtained from the windows is in agreement with reasonable extrapolations of all other penetration experiments. The cumulative flux-mass curve determined by the penetration experiments is in good agreement with the zodiacal light measurements.

REFERENCES

BONNER, G. P., HEIDT, M. F., KOTILA, C. L., LINTOTT, J. A., NOVOTNY, J. E., SHAFER, J. W. and STOKES, R. C. (1968). Postflight optical evaluation of the right-hand and left-hand windows of Gemini missions 4, 5, 6 and 7. *NASA Tech. Note* No. D-4916.

DOHNANYI, J. S. (1966). Model distribution of photographic meteors. *Bellcomm, Inc: Tech. Rep.* No. 66-340-1.

GAULT, D. E., SHOEMAKER, E. M. and MOORE, H. J. (1963). Spray ejected from the lunar surface by meteoroid impact. *NASA Tech. Note* No. D-1767.

JENNISON, R. C., MCDONNELL, J. A. M. and RODGERS, I. (1967). The Ariel II micrometeorite penetration measurements. *Proc. R. Soc.* **A300**.

MCCRACKEN, C. W., ALEXANDER, W. M. and DUBIN, M. (1961). Direct measurements of interplanetary dust particles in the vicinity of the Earth. *NASA Tech. Note* No. D-1174.

NAUMANN, R. J. (1966). The near-Earth meteoroid environment. *NASA Tech. Note* No. D-3717.

VERNIANI, F. and HAWKINS, G. S. (1965). Masses, magnitudes and densities of 320 radio meteors. *Harvard College Obs. Smithson. Astrophys. Obs. Radio Meteor Project Res. Rep.* No 12.

WHIPPLE, F. L. (1963). On meteoroids and penetration. *J. geophys. Res.* **68**, 4929.

WHIPPLE, F. L. (1967). On maintaining the meteoritic complex. *Smithson. Astrophys. Obs. Spec. Rep. No.* 239.